Pulse splitting in the anomalous group-velocity-dispersion regime

Samuel E. Schrauth,[1,*] Bonggu Shim,[1] Aaron D. Slepkov,[1] Luat T. Vuong,[1] Alexander L. Gaeta,[1] Nir Gavish,[2] and Gadi Fibich[2]

[1]*School of Applied and Engineering Physics, Cornell University, Ithaca, New York, 14853, USA*

[2]*School of Mathematical Sciences, Tel Aviv University, Tel Aviv 69978, Israel*

[*]*ss575@cornell.edu*

Abstract: We investigate experimentally the role that the initial temporal profile of ultrashort laser pulses has on the self-focusing dynamics in the anomalous group-velocity dispersion (GVD) regime. We observe that pulse-splitting occurs for super-Gaussian pulses, but not for Gaussian pulses. The splitting does not occur for either pulse shape when the GVD is near-zero. These observations agree with predictions based on the nonlinear Schrödinger equation, and can be understood intuitively using the method of nonlinear geometrical optics.

OCIS codes: (190.3270) Kerr effect; (190.5530) Pulse propagation and temporal solitons; (190.5940) Self-action effects; (190.7110) Ultrafast nonlinear optics.

References and links

1. R. Y. Chiao, E. Garmire, and C. H. Townes, "Self-trapping of optical beams," Phys. Rev. Lett. **13**, 479–482 (1964).
2. N. A. Zharova, A. G. Litvak, T. A. Petrova, A. M. Sergeev, and A. D. Yunakovskii, "Multiple fractionation of wave structure in a nonlinear medium," Pis'ma Zh. Eksp. Teor. Fiz. **44**, 13–17 (1986).
3. S. N. Vlasov, L. V. Piskunova, and V. I. Talanov, "Three-dimensional wave collapse in the nonlinear Schrödinger equation model," Zh. Eksp. Teor. Fiz. **95**, 1945–1950 (1989).
4. A. L. Gaeta, "Catastrophic collapse of ultrashort pulses," Phys. Rev. Lett. **84**, 3582–3585 (2000).
5. A. Couairon and A. Mysyrowicz, "Femtosecond filamentation in transparent media," Phys. Rep. **441**, 47–189 (2007).
6. J. E. Rothenberg, "Pulse splitting during self-focusing in normally dispersive media," Opt. Lett. **17**, 583–585 (1992).
7. G. Fibich, V. M. Malkin, and G. C. Papanicolaou, "Beam self-focusing in the presence of a small normal time dispersion," Phys. Rev. A **52**, 4218–4228 (1995).
8. J. K. Ranka, R. W. Schirmer, and A. L. Gaeta, "Observation of pulse splitting in nonlinear dispersive media," Phys. Rev. Lett. **77**, 3783–3786 (1996).
9. S. A. Diddams, H. K. Eaton, A. A. Zozulya, and T. S. Clement, "Amplitude and phase measurements of femtosecond pulse splitting in nonlinear dispersive media," Opt. Lett. **23**, 379–381 (1998).
10. A. A. Zozulya, S. A. Diddams, A. G. Van Engen, and T. S. Clement, "Propagation dynamics of intense femtosecond pulses: multiple splittings, coalescence, and continuum generation," Phys. Rev. Lett. **82**, 1430–1433 (1999).
11. A. A. Zozulya, S. A. Diddams, and T. S. Clement, "Investigations of nonlinear femtosecond pulse propagation with the inclusion of Raman, shock, and third-order phase effects," Phys. Rev. A **58**, 3303–3310 (1998).
12. S. Tzortzakis, L. Sudrie, M. Franco, B. Prade, A. Mysyrowicz, A. Couairon, and L. Bergé, "Self-guided propagation of ultrashort IR laser pulses in fused silica," Phys. Rev. Lett. **87**, 213902 (2001).
13. K. D. Moll and A. L. Gaeta, "Role of dispersion in multiple-collapse dynamics," Opt. Lett. **29**, 995–997 (2004).
14. M. Trippenbach and Y. B. Band, "Effects of self-steepening and self-frequency shifting on short-pulse splitting in dispersive nonlinear media," Phys. Rev. A **57**, 4791–4803 (1998).

#142925 - $15.00 USD
Received 18 Mar 2011; accepted 17 Apr 2011; published 26 Apr 2011

15. S. Skupin and L. Bergé, "Self-guiding of femtosecond light pulses in condensed media: Plasma generation versus chromatic dispersion," Physica D **220**, 14–30 (2006).
16. J. Liu, R. Li, and Z. Xu, "Few-cycle spatiotemporal soliton wave excited by filamentation of a femtosecond laser pulse in materials with anomalous dispersion," Phys. Rev. A **74**, 043801 (2006).
17. G. Fibich, N. Gavish, and X. Wang, "Singular ring solutions of critical and supercritical nonlinear Schrödinger equations," Physica D **231**, 55–86 (2007).
18. N. Gavish, G. Fibich, L. T. Vuong, and A. L. Gaeta, "Predicting the filamentation of high-power beams and pulses without numerical integration: a nonlinear geometrical optics method," Phys. Rev. A **78** 043807 (2008).
19. T. D. Grow, A. A. Ishaaya, L. T. Vuong, A. L. Gaeta, N. Gavish, and G. Fibich, "Collapse dynamics of super-Gaussian beams," Opt. Express **14**, 5468–5475 (2006).
20. A. M. Weiner, J. P. Heritage, and E. M. Kirschner, "High-resolution femtosecond pulse shaping," J. Opt. Soc. Am. B **5**, 1563–1572 (1998).
21. J. K. Ranka, A. L. Gaeta, A. Baltuska, M. S. Pshenichnikov, and D. A. Wiersma, "Autocorrelation measurement of 6-fs pulses based on the two-photon-induced photocurrent in a GaAsP photodiode," Opt. Lett. **22**, 1344–1346 (1997).

With the advent of ultrashort lasers, the study of high intensity light interactions with matter became possible. A high-power laser pulse will experience an intensity-dependent refractive index, which can result in self-focusing if the power P of a laser pulse is greater than a certain critical power P_{cr}. Although much of the initial work dealt with spatial effects, the dynamics of spatio-temporal wave collapse has generated significant interest [1–3] and includes a broad range of phenomena including pulse compression, pulse-splitting, supercontinuum generation, harmonic generation, plasma formation, and filamentation [4, 5]. One of the fundamental dynamical effects that arises from the interplay of nonlinearity and normal group-velocity dispersion (GVD) is pulse-splitting [2,3,6,7], which was demonstrated experimentally [8–13]. In the anomalous-GVD regime, temporal dynamics during beam collapse has not been extensively explored [14–16], and it was generally believed that the pusle should exhibit full spatio-temporal collapse.

Recent investigations of the spatial dynamics of a collapsing super-Gaussian beam show a behavior distinct from that for a Gaussian beam. Theory predicts that as the beam self-focuses the transverse profile evolves initially to a ring solution [17, 18], which was confirmed experimentally [19]. These results provided compelling evidence for the role of the initial beam shape on the spatial collapse dynamics, and motivated the development of the nonlinear geometrical optics (NGO) method for analyzing beam collapse without the need for full integration of the 3-D nonlinear Schödinger equation [18]. Two key NGO predictions are that the initial temporal dynamics in the anomalous-GVD regime is decoupled from the spatial dynamics and that it should depend on the temporal pulse shape in a manner entirely analogous to that exhibited in the spatial regime.

In this work we confirm these predictions experimentally, by propagating ultrashort pulses in the anomalous-GVD regime in a fused-silica sample at powers several times P_{cr}. We observe that temporal super-Gaussian input pulses undergo pulse-splitting, whereas Gaussian ones do not. To the best of our knowledge, no previous experimental work has shown that the temporal dynamics depend on whether or not the input pulse is temporally flat-top. We also find that no pulse-splitting occurs at the zero-GVD regime, regardless of the initial pulse shape.

We simulate pulse propagation using the nonlinear Schrödinger equation (NLSE) with dispersion for the slowly-varying envelope $A(\eta,\xi,\tau)$ centered at frequency ω,

$$\frac{\partial A}{\partial \zeta} = \frac{i}{4}\left(\frac{\partial^2}{\partial \eta^2}+\frac{\partial^2}{\partial \xi^2}\right)A - i\mathrm{sgn}(\beta_2)\frac{L_{df}}{2L_{ds}}\frac{\partial^2 A}{\partial \tau^2} + i\frac{L_{df}}{L_{nl}}|A|^2 A, \tag{1}$$

where w_0 is the spot size, $L_{df} = kw_0^2/2$ is the diffraction length, $L_{nl} = (n_2 n_0 \omega |A_0|^2/2\pi)^{-1}$ is the nonlinear length, $|A_0|$ is the magnitude of the input laser field, $\eta = x/w_0$ and $\xi = y/w_0$ are

#142925 - $15.00 USD Received 18 Mar 2011; accepted 17 Apr 2011; published 26 Apr 2011

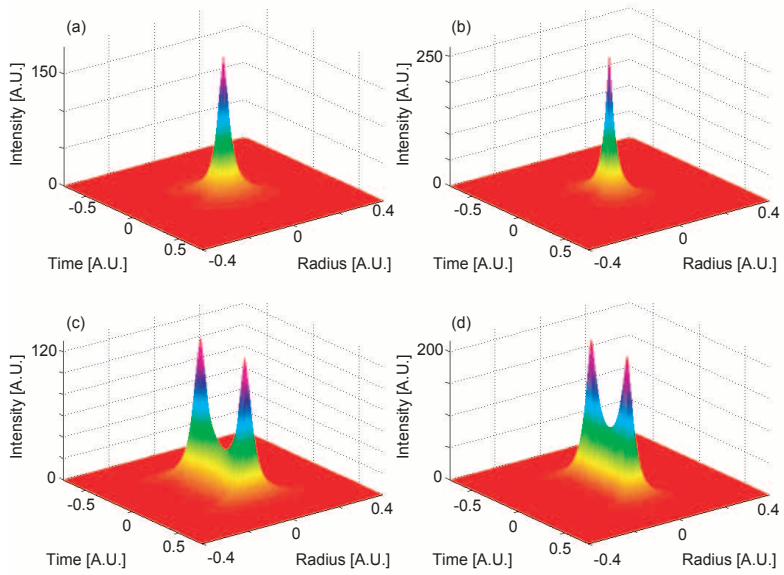

Fig. 1. Comparison of simulation results for Gaussian temporal profile (top) and super-Gaussian temporal profile (bottom), for input power of $2P_{cr}$ [(a) and (c)], $3P_{cr}$ [(b) and (d)], wavelength of 1550 nm, and β_2 of -279 fs^2/cm. The input spatial profiles for all simulations are Gaussian. The spatio-temporal profiles are taken from the propagation point at which the beam is collapsing and before the intensity becomes sufficiently high that higher order effects change the dynamics.

the normalized coordinates, $\zeta = z/L_{df}$ is the normalized propagation length, τ_p is the temporal pulse width, $L_{ds} = \tau_p^2/|\beta_2|$ is the dispersion length, $\tau = [t - (z/v_g)]/\tau_p$ is the normalized retarded time for the pulse traveling at the group velocity v_g. Figure 1 shows simulations of the NLSE [Eq. (1)]. All simulations have a Gaussian spatial profile $\exp(-r^2)$ as the input, while the temporal profile is varied. The value of L_{df}/L_{ds} for all simulations is 0.04. Two cases of the collapse of a Gaussian pulse $\exp(-t^2)$ are shown in the top part of the figure. Figure 1(a) is $2P_{cr}$ and Fig. 1(b) is $3P_{cr}$. Overall the temporal dynamics result in 3-D collapse as predicted by previous work. However, for a super-Gaussian temporal profile $\exp(-t^4)$, the pulse undergoes splitting, as shown in Fig. 1(c) for $2P_{cr}$ and Fig. 1(d) for $3P_{cr}$. In the spatial domain all input profiles are a Guassian, and therefore they evolve into a peak-type profile.

The pulses dynamics can be explained intuitively by the NGO method [18], which approximates the initial self-focusing dynamics with a reduced system of linear ordinary differential equations. These equations show that initially, the spatial and temporal dynamics are decoupled. The temporal dynamics in the anomalous-GVD regime is governed by the NGO eikonal equation for the ray trajectories,

$$\frac{dT(z)}{dz} = 2z\frac{d}{dT}|\psi_0(T)|^2, \tag{2}$$

and by the NGO transport equation for amplitude evolution along the rays,

$$\frac{dC(z)}{dz} = -C[T(z)]z\frac{d^2}{dT^2}|\psi_0(T)|^2, \tag{3}$$

#142925 - $15.00 USD Received 18 Mar 2011; accepted 17 Apr 2011; published 26 Apr 2011

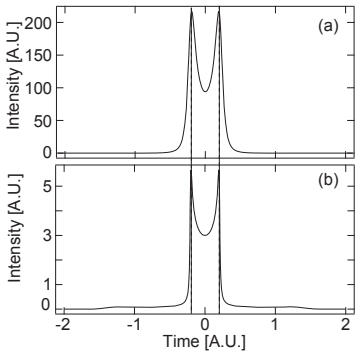

Fig. 2. Comparison of simulation results for a super-Gaussian temporal profile. The top (a) is the on-axis temporal profile found by directly integrating the NLSE in the anomalous (a) with input power $3P_{cr}$, wavelength of 1550 nm, and β_2 of -279 fs^2/cm. The bottom (b) is found using the 1-D building block of the NGO method. Although the profiles are slightly diffrerent, the peaks of the split pulses occur at ± 0.2 for both direct integration and the NGO method.

where T is the temporal coordinate of the ray at the propagation distance z, ψ_0 is the input field and C is the z-dependent amplitude. Equations (2) and (3) show that for a high-power temporal profile of the form $\exp(-t^{2m})$, the pulse will undergo splitting if $m > 1$, but will focus to a single peak if m = 1 [18], as is confirmed in direct numerical simulations of the NLSE, see Fig. 1. Comparison of the on-axis temporal profile for m = 2 (temporal super-Gaussian), shows a remarkable agreement between the solutions of the NLSE [Eq. (1)] and of the NGO equations [Eqs. (2) and (3)], see Fig. 2. Note that the peaks of the split pulses are at the same temporal position $\tau = \pm 0.2$.

We performed experiments to investigate these predictions with an amplified Ti:sapphire laser system operating at 800 nm, which generates 1.6-mJ, 70-fs pulses at a 1-kHz repetition rate. The output of the amplified system pumps an optical parametric amplifier to produce 150-μJ pulses at 1510 nm or 125-μJ pulses at 1275 nm. These two wavelengths are chosen since they correspond to the anomalous-GVD and the zero-GVD regimes, respectively, for the fused-silica sample. We spatially filter the output and temporally shape the pulse using a standard 4-f pulse shaper [20] with a 1-D double-mask liquid-crystal spatial light modulator to tailor the amplitude and phase of the spectrum. The output of the pulse shaper has pulse durations of 200-fs and 160-fs at 1510 nm and 1275 nm, respectively. We focus the outputs of the pulse shaper onto the front face of the sample, with spot sizes of 245 μm and 185 μm for 1510 nm and for 1275 nm, respectively. We use a 30-mm fused-silica sample, for which the physical parameters are as follows: at 1510 nm β_2 = -279 fs^2/cm and $n_2 = 2.2\times10^{-16}$ cm^2/W, and at 1275 nm β_2 = 1 fs^2/cm and $n_2 = 2.5\times10^{-16}$ cm^2/W [15]. Upon propagation through the sample, we use a two-photon autocorrelator [21] and an optical spectrum analyzer as diagnostics.

The autocorrelation of the pulse for various powers after propagation through the 30-mm fused-silica sample is shown in Fig. 3. The traces in Fig. 3(a) are the autocorrelations for a temporal Gaussian input profile through the sample. The energy increases from the bottom to the top trace. As the energy is increased, there is no indication of any pulse-splitting. The traces in Fig. 3(b) are the autocorrelations for a temporal super-Gaussian input through the sample. They exhibit pulse splitting at the lowest peak power as evidenced by the appearance of shoulders on the autocorrelation trace, and as the energy is increased the pulse-splitting becomes more pronounced. These observations are consistent with our theoretical predictions.

#142925 - $15.00 USD Received 18 Mar 2011; accepted 17 Apr 2011; published 26 Apr 2011

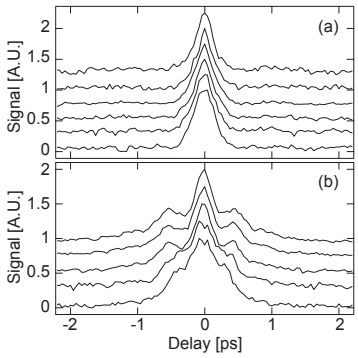

Fig. 3. Autocorrelation traces after propagation through 30 mm of fused silica at a wavelength of 1510 nm. The top plot (a) is for a temporal Gaussian input profile with peak power increasing from bottom to top (P = 15.7 MW, 24.7 MW, 33.7 MW, 41.5 MW, 49.4 MW, 62.8 MW). The lower plot (b) is for a temporal super-Gaussian input profile with peak power increasing from bottom to top (P = 11.2 MW, 14.6 MW, 18.0 MW, 21.8 MW, 26.9 MW). For the super-Gaussian case the pulse-splitting is pronounced as the power is increased.

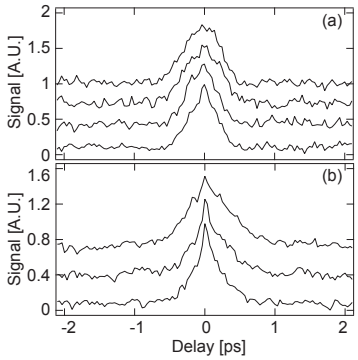

Fig. 4. Pulse autocorrelation traces after propagation through 30-mm of fused-silica at wavelength of 1275 nm. The top plot (a) is for a temporal Gaussian input profile with power increasing from bottom to top (P = 33.8 MW, 50.7 MW, 67.6 MW, 84.5 MW). The lower plot (b) is for a temporal super-Gaussian input profile with power increasing from bottom to top (P = 19.7 MW, 29.6 MW, 45.1 MW). Pulse-splitting does not occur in either case.

As a comparison, we also perform the analogous experiment with pulses at 1275 nm, at which point the GVD is nearly zero (i.e., β_2 = 1 fs^2/cm). As expected, we do not observe pulse-splitting at this wavelength for either a Gaussian pulse [Fig. 4(a)] or for a super-Gaussian pulse [Fig. 4(b)] for the range of powers studied, which indicates that the pulse-splitting of super-Gaussian pulses should only occur in the anomalous-GVD regime, as predicted.

In conclusion, we show that the spatio-temporal dynamics strongly depends on the temporal profile of the pulse. We observe that pulse-splitting can occur in the anomalous-GVD regime for the case of super-Gaussian input pulses, which confirms recent theoretical predictions. This splitting can be interpreted as a temporal focusing of the energy in the beam due to strong self-phase modulation, and is analogous to the spatial focusing of the beam to a ring profile for a

#142925 - $15.00 USD Received 18 Mar 2011; accepted 17 Apr 2011; published 26 Apr 2011

super-Gaussian spatial profile [17–19]. These results are relevant to understanding how shaping the temporal profile of the initial pulse can dramatically change the temporal dynamics and the filamentation and plasma formation process. Finally, we note that this splitting is very different from the one in the normal-GVD regime. Indeed, in the normal GVD regime, both Gaussian and super-Gaussian pulses undergo a temporal splitting. Moreover, this temporal splitting strongly depends on the spatial dynamics, since it only occurs after the pulse undergoes a significant spatial self-focusing, and it is associated with a departure from a self-similar Townes spatial profile [7].

Acknowledgments

This work was supported by the National Science Foundation (NSF) under Grant No. PHY-0703870, the United States Army Research Office (USARO) under Grant No. 186695-PH, and the United States Air Force Office of Scientific Research (USAFOSR) under grant FA9550-10-1-0561. This research was partially supported by Grant No. 2006-262 from the United States-Israel Binational Science Foundation (BSF), Jerusalem, Israel.

#142925 - $15.00 USD Received 18 Mar 2011; accepted 17 Apr 2011; published 26 Apr 2011